Neurobiology of Stress 15 (2021) 100358

Contents lists available at ScienceDirect

Neurobiology of Stress

journal homepage: www.elsevier.com/locate/ynstr

Activation of 6–8-week-old new mature adult-born dentate granule cells contributes to anxiety-like behavior

Guohua Wang [b], Canmao Wang [c], He Chen [d], Limei Chen [d], Juan Li [a,*]

[a] School of Basic Medical Sciences, Southern Medical University, Guangzhou, 510515, China
[b] 502 Room, 28 Yunjing Road, Guangzhou, 510515, China
[c] Department of Pharmacy, Nanfang Hospital, Southern Medical University, Guangzhou, 510515, China
[d] Department of Histology and Embryology, School of Basic Medical Sciences, Southern Medical University, Guangzhou, 510515, China

ARTICLE INFO

Keywords:
Anxiety
New mature adult-born dentate granule cells
Hyperactivity
Learning and memory
Quiet property

ABSTRACT

Adult-born dentate granule cells (aDGCs) at 4–6 weeks of age are particularly excitable but subsequently develop the quiet properties of mature cells. Most existing studies have focused on the hyperactivity of 4–6-week-old aDGCs or neurogenesis, which confers stress resilience or buffers stress responses. However, the function of the quiet property of new mature aDGCs remains unclear. Here we used a retrovirus expressing cre recombinase in combination with an associated-adenovirus to specifically interfere with the activity of new mature aDGCs, and estimated anxiety-like behaviors by the open-field test and elevated plus maze test, antidepressant-like behaviors by the tail suspension test, and spatial memory by the Barnes maze test. We found that sustained hyperactivity of 6–8-week-old, but not 8–10-week-old, aDGCs induced anxiety-like behaviors, and suppression of the activity of 6–8-week-old aDGCs disturbed spatial memory. Meanwhile, sustained hyperactivity of 6–8-week-old aDGCs induced activation of mature dentate gyrus (DG) neurons and inhibition of immature aDGCs. Additionally, the mice showing anxiety-like behaviors induced by chronic mild immobilization stress exhibited increased activity in 6–8-week-old aDGCs. Furthermore, the sustained hyperactivity of mature DG neurons also induced anxiety-like behaviors and decreased the activity of immature aDGCs. Our results combined show that the excitation of 6–8-week-old new mature aDGCs, which prohibits them from normally entering the resting state, determines anxiety-like behavior, while the maintenance of normal excitation ability of 6–8-week-old new mature aDGCs confers memory. Our results suggests that strategies aimed at inhibiting unusual hyperactive new mature aDGCs at a restricted time window may protect against stress-related psychiatric disorders, such as anxiety and depression.

1. Introduction

Adult hippocampal neurogenesis exists in rodents, humans, and non-human primates (Horgusluoglu et al., 2017; Kuhn et al., 2018; Park, 2019; Planchez et al., 2020; Snyder et al., 2011; Toda et al., 2019), which has been proved to be essential for stress-resilience and antidepressant action in rodents (Anacker et al., 2018; Planchez et al., 2020; Snyder et al., 2011; Tunc-Ozcan et al., 2019). During new-born neurons integration into neural networks, hippocampal neurogenesis follows the immature and mature stages, which have different morphological and electrophysiological characteristics in rodents (Kropff et al., 2015; Ohline et al., 2018; Piatti et al., 2011; Toda et al., 2019). Usually, adult-born dentate granule cells (aDGCs) at 4–6 weeks of age show enhanced plasticity compared to other stages (Ge et al., 2007), and are particularly excitable but subsequently develop the quiet properties of mature cells (Kropff et al., 2015; Ohline et al., 2018; Piatti et al., 2011). Therefore, aDGCs may play different roles in physiological processes and disease status in different time window.

Most existing studies have focused on the properties of ~6-week-old aDGCs, reporting that the hyperactivity of 4–6-week-old aDGCs protects the body against depressive- and anxiety-like behaviors; for example, increased 0–6-week hippocampal neurogenesis confers stress resilience or buffers stress responses, with activated aDGCs at 4 weeks of age suppressing depressive- and anxiety-like behaviors, while silencing the 0–6-week adult-born neurons promotes stress susceptibility in mice (Anacker et al., 2018; Snyder et al., 2011; Tunc-Ozcan et al., 2019).

* Corresponding author.
E-mail address: lijuan860103@163.com (J. Li).

https://doi.org/10.1016/j.ynstr.2021.100358
Received 16 February 2021; Received in revised form 17 June 2021; Accepted 17 June 2021
Available online 20 June 2021

Another research show that silencing ~4-week-old, but not 2– or 8-week-old, aDGCs disrupted retrieval of hippocampal memory in mice (Gu et al., 2012). Although these studies have focused on the particularly excitable and highly plastic aDGCs within 6 weeks, the function of the quiet property of new mature aDGCs (6–8 weeks) integrated into neural networks in mice remains unclear.

In the hippocampal dentate gyrus (DG) of mice, aDGCs can be divided into several stages according to their morphological and electrophysiological characteristics (Kerloch et al., 2019; Piatti et al., 2011). Only 4–5-week-old abGCs, but neither old aDGCs nor mature GCs, responded to stimulation with a remodeling of their dendritic arbor (Beining et al., 2017). Axonal projections of newborn neurons reach the CA3 area 10–11 days after viral infection, 5–6 days before the first spines are formed, and the peak of spine growth occurs during the first 3–4 weeks (Kerloch et al., 2019; Zhao et al., 2006). Meanwhile, adult-born neurons labeled by retrovirus in septal pole of hippocampus stop expressing DCX and start expressing NeuN within 3-week-old, and adult-born neurons labeled by retrovirus in temporal pole of hippocampus reach initial maturation after 4-week-old. Meanwhile, all new neurons were equally and completely matured within 8-week-old (Piatti et al., 2011; van Praag et al., 2002). Therefore, we defined 6–8 weeks aDGCs as new mature aDGCs, and aDGCs over 8 weeks as mature aDGCs.

We used chemogenetic techniques to selectively manipulate the activity of new mature aDGCs (6–8 and 8–10 weeks) and mature DG neurons, to characterize the function of the quiet property of new mature aDGCs (6–8 weeks and 8–10 weeks) and mature DG neurons in anxiety- and depressive-like behavior, spatial learning and memory, and the effect on the activity of young aDGCs or neurogenesis.

2. Material and methods

2.1. Mice

Male C57BL/6J mice (3–4 weeks old) were purchased from the Southern Medical University Animal Center (Guangzhou, China). All mice were acclimated to the experimenter for 4 weeks, while mice reached adult age (>7–8-week-old) (Gu et al., 2012), before proceeding to the virus injection. Mice were housed five per cage under standard conditions with *ad libitum* access to rodent chow and water and a 12:12-h light/dark cycle (lights on at 8:00 a.m.). All behavioral tests were conducted during the light period.

All efforts were made to minimize animal suffering and reduced the number of animals used for the study. All animal experiments were carried out in accordance with the National Institutes of Health guide for the care and use of Laboratory animals (NIH Publications No. 8023, revised 1978) and were approved by the Institutional Animal Care and Use Committee of the Southern Medical University.

2.2. Viral constructs

Retrovirus (ROV-GFP and ROV-cre) and associated-adenovirus (AAV2/9-hsyn-DIO-hM3Dq-mCherry-WPRE-pA, AAV2/9-hsyn-DIO-hM4Di-mCherry-WPRE-pA, AAV2/9-hSyn-hM3Dq-mCherry-WPRE-pA, and AAV2/9-hSyn-hM4Di-mCherry-WPRE-pA) were packaged and supplied by the Shanghai Taitool Bioscience Co. Ltd. at a titer of 2×10^8 viral genomes (v.g.) per mL or 1×10^{13} v. g./mL, respectively. The final concentrations in the ROV and AAV cocktails for injections were 1.6×10^8 v. g./mL and 2×10^{12} v. g./mL, respectively.

2.3. Stereotactic surgeries and viral injections

For all surgical procedures, mice were anesthetized with 1.5% isoflurane at an oxygen flow rate of 1 L/min and positioned in a stereotaxic frame (Stoelting Instruments) on a warm pad. Eyes were lubricated with an ophthalmic ointment. Fur was shaved, and the incision site was sterilized with betadine/ethanol swabs before surgery. Subcutaneous carprofen (5 mg/kg) was provided perioperatively and for three days postoperatively for analgesia.

For ROV and AAV cocktail injections into the DG, 1 μL of the virus cocktail was bilaterally injected with a 5-μL Hamilton syringe with a 33-gauge flat needle at a constant speed of 100 nL/min. Virus was injected bilaterally at −2.18 mm AP, ±1.4 mm ML, and −2.1 mm DV. After each injection, the needle was left at the injection site inside the brain for an additional 5 min to aid diffusion from the needle tip and to prevent backflow. The needle was then slowly retracted and the scalp incision closed with stylolite. Each mouse was monitored and received carprofen (subcutaneous, 5 mg/kg) for pain management for three days after surgery. Mice were housed for 6 or 8 weeks postoperatively before the start of the BMT or for 6 weeks before the onset of chronic mild immobilization stress (CMIS) to allow for recovery from surgery and sufficient viral expression.

2.4. Clozapine administration

For in vivo activation or silencing of new mature aDGCs or mature granule cells (GCs) in the DG of mice, clozapine (Tocris, # 0444) was dissolved in 100% dimethyl sulfoxide (DMSO) and diluted with 0.9% saline to a final concentration of 0.04 mg/mL clozapine and 0.001% DMSO. A volume of 0.4 mg/kg clozapine was injected intraperitoneally every day 45 min before each habituation, acquisition, and test session during behavioral test.

2.5. Chronic mild immobilization stress

Stressed animals were put into the tube (diameter, 3.5 cm), and the plug was inserted into the tube a little more loosely, which allowed the mice to move slightly inside the tube. Mice underwent 2–3 h of CMIS each day for 10 consecutive days before behavioral testing. Non-stressed animals remained in their home cages before experimentation.

2.6. Behavioral tests schedules

We used a battery of behavioral tests, including Barnes maze test (BMT), open field test (OFT), elevated plus maze test (EPMT), and tail suspension test (TST). Mice received only one training or test procedure each day without rest days, BMT was performed first, followed by the OFT, EPMT, and TST. All behavioral tests were performed during lighting conditions. The activity of mice during the behavioral test was recorded by Anymaze software (Stoelting) and exhibited by heatmaps, which were generated by the mean heat map of the group's center point to indicate the mean activity of all animals of each group.

2.7. Barnes maze test

Dry-land (Barnes) maze tests were performed as previously described to assess the spatial memory with modification (Attar et al., 2013; Awasthi et al., 2019; Kurawa et al., 2020; Pitts, 2018; Rosenfeld and Ferguson, 2014). The Barnes maze consisted of a white circular platform (diameter, 92 cm; 50 cm above the ground), with 20 equally spaced holes (diameter 5 cm) along the edge. Three visual cues (26×26 cm^2 in size) were placed 5 cm away from the platform edge. The escape chamber ($15.5 \times 9 \times 6$ cm^3) was placed under the target hole. The maze was placed in the center of a room, and two 150-Watt LED lights were placed on the top of the maze, with the camera between the two lamps. After testing each mouse, the whole maze was cleaned with 75% ethanol to eliminate olfactory cues. For each trial, the mouse was placed inside the center tube, the tube was covered for 15 s, after which the cover was gently lifted away from the center tube, and then the recording was initiated. The BMT was conducted in three phases: habituation (1 day), acquisition training (2–4 days or 6–8 days), and probe trial (day 5 or 9). During habituation, mice were habituated to the maze by placing them in a clear plastic cylinder (15 cm in diameter) in the middle of the

platform for 30 s before gently guiding them to the target hole, where they were given 3 min to enter the escape chamber. If the mice did not enter the escape chamber, they were gently nudged with the cylinder into the chamber. All mice spent 1 min in the escape chamber before being returned to their home cage. For acquisition training, each trial, lasting 2 min, was initiated after lifting the cylinder. If the mouse climbed into the escape chamber, the trial was stopped, and the mouse returned to its home cage after remaining inside the escape chamber for 1 min. If the mouse did not climb into the escape chamber within 2 min, it was gently guided to the target hole with the clear plastic cylinder and given 3 min to climb into the escape chamber, where it remained for 1 min, before being returned to its home cage. In the probe trial, the escape chamber was removed, and mice were allowed to explore the maze for 2 min. Three-point (head, center, tail) tracking data were monitored and analyzed by Anymaze software (Stoelting). The latency (the time used before the first arrival at the target hole) and active time at the target hole (the total time of the mice head entered at range < 5.5 cm around the central point of the target hole within 2 min) were used to explore spatial learning and memory.

2.8. Open field test

Anxiety-like behaviors were evaluated using OFT as described in 2.6 (Anacker et al., 2018; Vu et al., 2018). After the BMT or CMIS procedure, mice were placed in an open field arena (40 cm $\times$ 40 cm $\times$ 40 cm) at 650 lux for 5 min. Behavior was recorded with Anymaze software (Stoelting), and the time mice spent in the center of the open field arena (20 cm $\times$ 20 cm), as well as the total distance traveled, were analyzed.

2.9. Elevated plus maze test

After OFT, the EPMT was performed as described in 2.6 (Autry et al., 2011; Wang et al., 2013). Mice were introduced into the center quadrant of a 4-arm maze with two open and two closed arms, facing to the open arms. Before every trial, urine was removed with Kimwipes, and the maze was cleaned with water and 75% ethanol. The procedure was recorded with Anymaze software (Stoelting) for 5 min. The number of entries into the open arms and the total active time spent in the open arms were analyzed.

2.10. Tail suspension test

After EPMT, the TST was performed as described in 2.6, to evaluate antidepressant-like activity (Can et al., 2012; Wang et al., 2013). The mouse was suspended with medical tape, with its nose 20–25 cm above the floor, and videotaped with a recording device during the entire test. The immobility time during a period of 5 min was measured by Anymaze software (Stoelting).

2.11. Bromodeoxyuridine labeling

After retrovirus + AAV injection, mice were injected with Bromodeoxyuridine (BrdU) (Selleck, S7918, dissolved in 0.9% NaCl) intraperitoneally at a dose of 100 μg/kg, after 6 weeks recovery, mice hippocampus tissue sections were pretreated with 2 N HCl for 45 min at room temperature (RT), then were used for BrdU immunofluorescence.

2.12. Immunofluorescence

Forty-five minutes following saline or clozapine injection, mice were anesthetized and transcardially perfused with phosphate buffered saline (PBS) followed by 4% paraformaldehyde. Brains were fixed overnight in 4% paraformaldehyde and then transferred to 30% sucrose for two days. Floating sections with a thickness of 25 μm were cut through the entire hippocampus on a cryostat (Leica CM3050S). Tissue sections were washed three times in PBS, blocked in 10% normal serum with 0.3% Triton X-100 in PBS for 1 h at RT, and incubated overnight at 4 °C in primary antibody diluted in 1% bovine serum albumin with 0.3% Triton X-100 in PBS. Sections were washed three times in PBS and then incubated for 1 h at RT with a fluorophore-conjugated secondary antibody (1:200; donkey anti mouse Alexa-405, donkey anti mouse Alexa-488, A21202; goat anti mouse Alexa-594, A11037; A48257; donkey anti rabbit Alexa-488, A21206; donkey anti rabbit Alexa-594, A32754; goat anti rabbit Alexa-647, A32733; goat anti chicken Alexa-488, A11039; goat anti guinea pig Alexa-488, A11073; goat anti guinea pig Alexa-594, A11076; goat anti guinea pig Alexa-647, A21450; Thermo Fisher) or 4′,6-diamidino-2-phenylindole (DAPI) for nuclear stain (Invitrogen, Carlsbad, CA, USA). After three final washes in PBS, floating sections were mounted with ProLong Gold Antifade Reagent (Life Technologies, Carlsbad, CA, USA). The primary antibodies used were as follows: chicken anti-GFP (1:2000, ab205402, Abcam), mouse anti-mCherry (1:500, ab125096, Abcam), rabbit anti-c-Fos (1:1000, ab222699, Abcam), guinea pig anti-Doublecortin (1:500, AB2253, Millipore), rabbit anti-Egr1 (1:500, #4153, Cell Signaling), mouse anti-NeuN (1:500, MAB377, Millipore), and mouse anti BrdU (1:1000, B2531, Sigma-Aldrich).

2.13. Confocal microscopy

To identify co-localization of mCherry, doublecortin (DCX), and NeuN, z-stacks of immunolabeled sections were obtained using a confocal scanning microscope (Zeiss LSM880, Germany). Z-stacks of the DG were obtained (step size: 2 μm) using sequential scanning to prevent bleed-through between fluorophores. Six Z-stacks of equal thickness and equivalent rostro-caudal position were quantified for each sample. Stereological cell counting was performed using ImageJ software. For per-volume quantification, cell counts were normalized to the volume of the DG granule cell layer. All imaging and quantification procedures were performed blinded to the experimental conditions.

2.14. Statistics

Statistical analyses were performed with Student's t-test, one-way ANOVA, or two-way ANOVA with Tukey's paired comparisons test for correction for multiple comparisons, as indicated in the Figures. SPSS and GraphPad Prism 8 software were used for the analyses. The significance threshold used was $P < 0.05$. The exact sample size for each experimental condition is represented in the Figures by a symbol. All data are reported as means ± standard error of the mean.

3. Results

3.1. Activation of 6–8-week-old new mature aDGCs, but not 8–10-week-old mature aDGCs, induce anxiety-like behavior, and silence 6–8-week-old new mature aDGCs decrease spatial memory

Some previous studies have used Nestin-creERT mice hybridized with hM4Di or bax transgenic mice or GFAP-TK mice to interfere with both immature and mature aDGCs, especially particularly excitable aDGCs (Anacker et al., 2018; Drew et al., 2016; Snyder et al., 2011; Tunc-Ozcan et al., 2019). To address our question about the function of the quiet property of new mature aDGCs (6–8 weeks), the key is to selectively interfere with the activity of 6–8-week new mature aDGCs. Retrovirus are useful for labeling new born neurons at distinct stages (Cole et al., 2020; Zhao et al., 2006), when combined with optogenetic or chemogenetic tools, they can specifically interfere with the activity of aDGCs at a specific time window (Gu et al., 2012; Kajimoto et al., 2016). Therefore, we used a retrovirus expressing cre recombinase to infect dividing neuronal stem cells, in combination with an AAV with the human synapsin I promoter (mature neuron promotor) and cre-on hM3Dq-mCherry or hM4Di-mCherry, which are theoretically only expressed in cre-expressing mature aDGCs; then, we performed the

subsequent assessments after 6 weeks to allow for maturation of aDGCs infected by both the retrovirus and AAV (Fig. 1a and b). By evaluating the co-immunofluorescence of mCherry with doublecortin (DCX, immature neuron marker) and NeuN (mature neuron marker) to identify the type of mCherry-positive neurons, we found that all mCherry-positive neurons were NeuN-positive mature neurons while being concurrently DCX-negative (Fig. 1c, n = 4 mice/279 neurons). In addition, all mCherry-positive neurons were labeled with BrdU injected at the time of retrovirus + AAV labelling (Fig. 1d, n = 4 mice/327 neurons). Our results indicated that our viral injection paradigm was successfully expressed in newly mature aDGCs.

To verify the effects of clozapine on the activity of new mature aDGCs in vivo, we examined the expression of the immediate-early gene c-Fos as a marker for neuronal activity (Jungenitz et al., 2014; Ohline et al., 2018; Tunc-Ozcan et al., 2019). Forty-five minutes after clozapine treatment (0.4 mg/kg), which shows higher DREADD (designer receptors exclusively activated by designer drugs) affinity and potency than clozapine N-oxide (Gomez et al., 2017), hM3Dq-mCherry-positive new mature aDGCs showed increased co-localized numbers of c-Fos labeled cells in the DG compared to the control, indicating an increase in the activity of new mature aDGCs, while hM4Di decreased the activity of new mature aDGCs compared to the control (Fig. 1e and f). Moreover, both hM3Dq and hM4Di groups had similar ratios between mCherry positive new mature aDGCs and DCX positive immature aDGCs to mCherry control group (Fig. 1g), which excluded the effects of different ratios between new mature aDGCs and immature aDGCs on the subsequent behavioral performance. These results indicate that we could successfully activate or silence new mature aDGCs within a specific time period.

Next, using our mouse model, we investigated the functions of the quiet property of new mature aDGCs (6–8 weeks old) in spatial learning and memory, depression, and anxiety. We used the BMT as a measure of

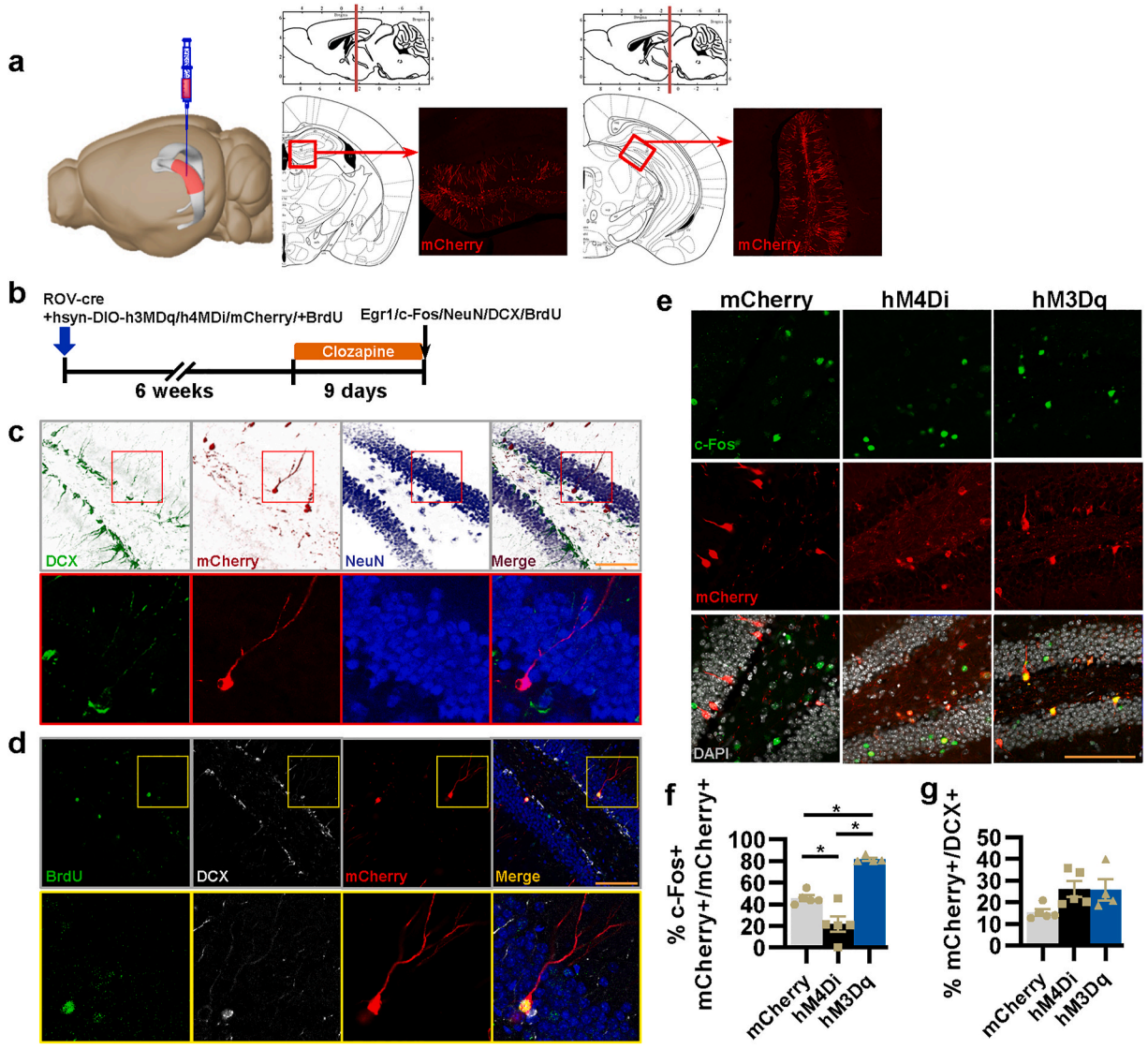

Fig. 1. ROV-cre combined human synapsin I promoter AAV successfully expressed in and interfered with the activity of new mature aDGCs. a, ROV-cre initiates the expression of mCherry fluorescence in the DG of mice. Image generated using the Allen Institute Brain Explorer 2 software (http://mouse.brain-map.org/static/brainexplorer). **b**, Experimental design for efficiency detection of virus tools. **c**, Confocal images of DCX, NeuN, mCherry, and GFP show the localization of mCherry-positive neurons. **d**, Confocal images of BrdU, DCX, mCherry, and DAPI show co-localization of BrdU- and mCherry-positive neurons. **e**, Confocal photographs of c-Fos, mCherry, GFP, and DAPI show the localization of c-Fos in mCherry-positive neurons. **f**, Quantification of the ratio of c-Fos and mCherry double-positive neurons to mCherry positive neurons in the DG following a series of clozapine treatments ($F_{2,11} = 37.069$, $^*P < 0.001$). **g**, Quantification of the ratio of mCherry -positive new mature neurons to DCX positive immature neurons in the DG following a series of clozapine treatments ($F_{2,11} = 3.438$, $P = 0.069$). All scale bars are 100 μm.

spatial learning and memory, the OFT and EPMT as measures of anxiety-like behaviors, and TST as a measure of antidepressant-like behavior (Ramirez et al., 2015) (Fig. 2a). The BMT results showed that the suppression of new mature aDGCs significantly decreased the time at the target hole in PT2 but had no effect on the latency to the target hole (Fig. 2b–d), indicating that spatial memory required activation of new mature aDGCs. Importantly, activation of new mature aDGCs significantly decreased the time in the center in OFT and the entries into the open arms in EPMT but had no effect on the total immobile time in TST and the total traveled distance in OFT (Fig. 2e-l). Meanwhile, although the control mice spent more time in the center of an open field than hM3Dq group (Fig. 2f), it did not affect the latency to and the time at the target hole compared with hM3Dq group in the BMT. Overall, our results indicated that continual activation of new mature aDGCs for several days by daily injections throughout the behavioral test can induce anxiety-like behavior but have no significant relevance to learning and memory, antidepressant-like behaviors, and motor ability. Furthermore, depressing the new mature aDGCs could damage memory without inducing anxiety- and antidepressant-like behavior.

Meanwhile, we also detected the quiet properties of 8–10-week-old mature aDGCs by extending the virus expression duration to 8 weeks before behavioral test (Fig. 3a). The BMT results showed that both activation and suppression of 8–10-week-old mature aDGCs did not affect the time at the target hole in PT2 and the latency to the target hole (Fig. 3b–d). Meanwhile, activation of 8–10-week-old mature aDGCs significantly decreased the total distance traveled in OFT but had no effect on the active time in the center of OFT, the entries into the open arms in EPMT, and the total immobile time in TST (Fig. 3e-l). Additionally, suppression of 8–10-week-old mature aDGCs increased the active time in the open arms of EPMT, but had no effect on the performance in OFT and TST. These results indicated that suppression of 8–10-week-old mature aDGCs increased the exploratory behavior, and activation of 8–10-week-old mature aDGCs did not induce the anxiety-like behavior, which further illustrated that 6–8-week stage of aDGCs was a key time window determining the emergence of anxiety-like behavior in mice.

3.2. Activation of 6–8-week-old new mature aDGCs, but not 8–10-week-old mature aDGCs, inhibit the activity of young aDGCs, and both increase the activity of mature GCs

Hippocampus plays a key role in cognition, stress responses and anxiety (Anacker and Hen, 2017; Anacker et al., 2018; Kheirbek et al., 2013). To investigate how the activation of 6–8-week-old new mature aDGCs affects the activity of the DG, we examined the expression of c-Fos. The number of c-Fos-positive cells selectively increased in the DG upon activation of new mature aDGCs in vivo (Fig. 2m and o). Many studies have reported a reduction in neurogenesis in several neurodegenerative disorders, such as Alzheimer's disease, anxiety, and depressive-like behavior (Anacker and Hen, 2017; Cho et al., 2015; Choi et al., 2018). Therefore, we examined immature neurons by assessing co-immunofluorescence of early growth response 1 (Egr1), which is upregulated by neuronal activity mainly in aDGCs (Jungenitz et al., 2014; Ohline et al., 2018; Tunc-Ozcan et al., 2019), with DCX, and we found that the activation of new mature aDGCs did not affect the number of immature aDGCs (Fig. 2n and q), but intriguingly decreased the activity of immature aDGCs (Fig. 2n and p), whose high excitability provides protection from depression and anxiety (Tunc-Ozcan et al., 2019). Meanwhile, we also detected the effect of 8–10-week-old mature aDGCs on the activity of the DG, and found that neither activation nor suppression of 8–10-week-old mature aDGCs affect the activity and the number of immature neurons (Fig. 3m–q). These results indicated that the activation of 6–8-week-old new mature aDGCs suppressed the activity of immature aDGCs, increased DG activity, and induced anxiety-like behavior.

3.3. The anxiety mice models exhibit increased activity in 6–8-week-old new mature aDGCs

Next, we further verified this conclusion using an anxiety mouse model. First, mice were infected with GFP retrovirus into the DG, and after waiting for 6 weeks until most of GFP + aDGCs became new mature aDGCs, mice were treated with 10 days of CMIS or spent time in a home cage. Subsequently, Egr1, DCX, and c-Fos immunostaining were used to detect the activity of immature aDGCs, new mature aDGCs, and mature GCs, while OFT, EPMT, and TST were conducted to assess the anxiety-like and antidepressant-like behaviors of the mice (Fig. 4a and b). We found that 10 days of CMIS induced a decrease in time in the center in OFT and the percentage of entries into the open arms in EPMT (Fig. 4i and j); it also increased the total distance traveled in OFT but did not affect the immobility time in TST, indicating that 10-day CMIS successfully induced anxiety-like behaviors, but not antidepressant like behavior, and induced a rebound rise in motor ability. On the other hand, the immunofluorescence results showed that CMIS increased the number of double Egr1+GFP + cells (Fig. 4g–f), indicating that CMIS increased the activity of **6–**8-week-old new mature aDGCs. Meanwhile, CMIS did not affect the number of c-Fos + mature GCs, Egr1+DCX + immature aDGCs, and DCX + cells in the DG of mice (Fig. 4g–f), further indicating that the abnormal excitation of 6–8-week-old new mature aDGCs had a correlative regulatory relationship with initiated anxiety-like behavior.

3.4. Activation of mature DG neurons also induced anxiety-like behavior

The DG provides a niche environment for neurogenesis (Navarro Negredo et al., 2020), and on the basis of the above results showing that the activation of new mature aDGCs increased the number of c-Fos + mature DG neurons, we further tested the function of mature DG neurons in spatial learning and memory, anxiety, and depressive mood. We directly interfered with mature DG neurons using hM3Dq and hM4Di AAV under an hsyn promoter (Fig. 5a and b). Clozapine treatment increased the number of c-Fos + cells in the hM3Dq group in the DG (Fig. 5d and e). This direct excitation resulted in reduced probe time, increased latency to the target hole (Fig. 6a–d), and reduced open field center exploration (Fig. 6e and f), which indicated that DG excitation could damage spatial learning capacity and memory and induce anxiety behavior. Moreover, DG excitation significantly increased the total traveled distance in OFT and the time in the open arms and the entries into the open arms in EPMT, while decreasing the total immobile time in TST, indicating that DG excitation increased motor ability and complex exploratory behavior in EPMT. Meanwhile, DG suppression had no significant effect on these behaviors (Fig. 6a–d). However, the immunofluorescence results showed that sustained excitation of mature GCs increased the number of c-Fos + cells (Fig. 6m and o) and decreased the number of Egr1+DCX + immature aDGCs and DCX + cells in the DG of mice (Fig. 6n, p, and q). Meanwhile, depression of mature GCs also decreased the number of Egr1+DCX + immature aDGCs. These data indicated that the normal activity of mature GCs provided a steady niche for neurogenesis and that the abnormal excitability of multitudinous mature GCs may induce the above complex behavioral performance. Overall, these data demonstrated that the behavioral effects of 6–8-week-old new mature aDGCs depend on the activity of part of mature DG neurons. Further detailed studies are required to identify these specific mature GCs.

4. Discussion

In this study, we used chemogenetic methods to evaluate the function of the quiet property of new mature aDGCs in anxiety- and depressive-like behavior, and spatial learning and memory. We found that activation of 6–8-week-old aDGCs contributes to anxiety-like behavior, while the maintenance of normal excitation ability of 6–8-

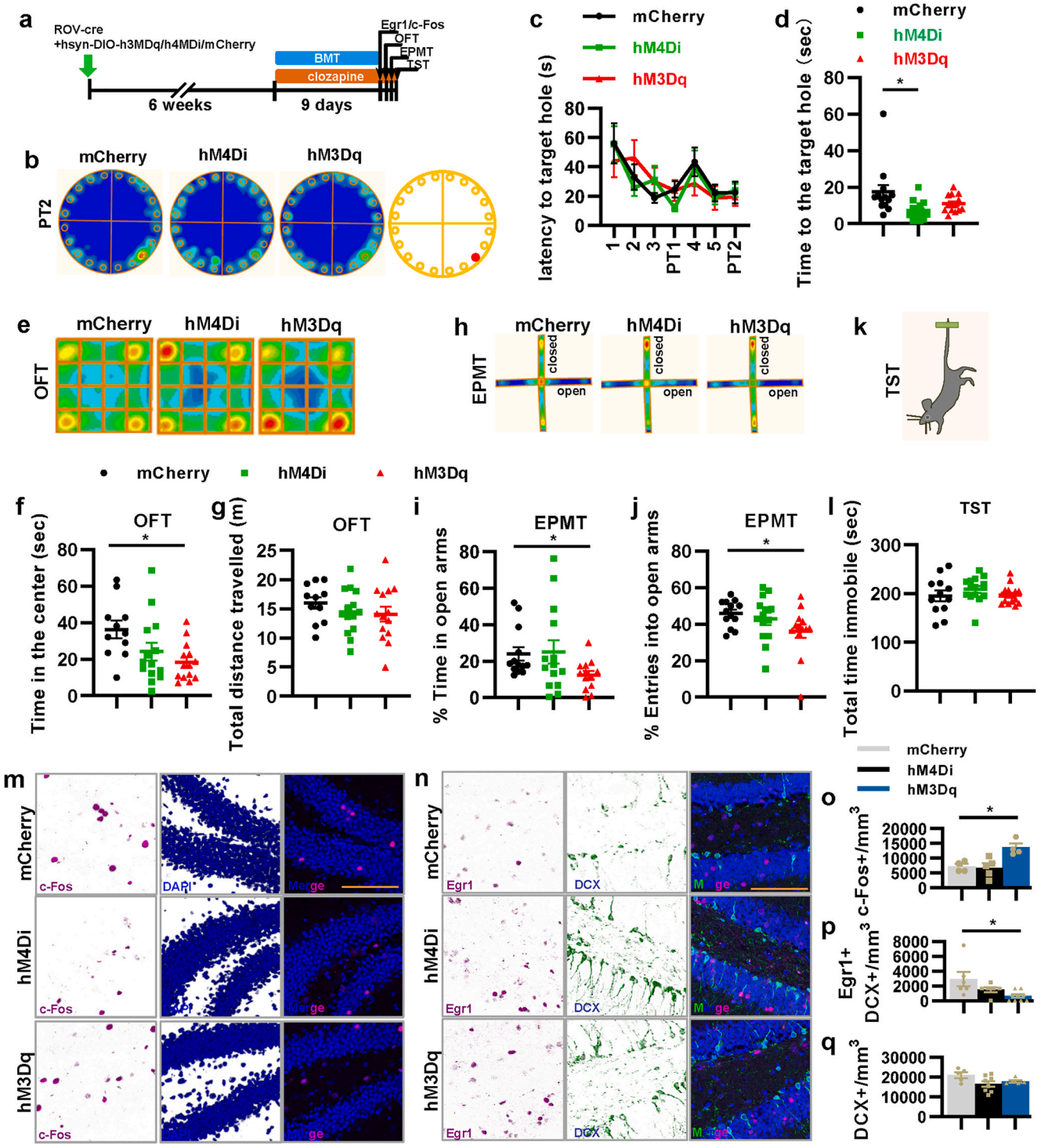

Fig. 2. The activity of 6–8-week-old new mature aDGCs regulates spatial memory, anxiety-like behavior, as well as the excitability of mature and immature aDGCs. a, Experimental design for the behavioral tests. BMT, Barnes maze test; OFT, open field test; EPMT, elevated plus maze test; and TST, tail suspension test. **b**, The heatmap of mice in probe test 2 of BMT. **c**, The latency to the escape hole in BMT during training and in probe tests 1 and 2 (two-way ANOVA, interaction $F_{12,265} = 0.723$, $P = 0.729$; day $F_{6,265} = 5.633$, $^*P < 0.001$; virus $F_{2,265} = 0.095$, $P = 0.909$). **d**, Active time at the escape hole ($F_{2,38} = 4.653$, $^*P = 0.016$). **e**, The heatmap of mice in OFT. **f**, Active time of mice in the center of OFT ($F_{2,36} = 4.422$, $^*P = 0.019$). **g**, Total distance traveled in OFT ($F_{2,36} = 0.749$, $P = 0.480$). **h**, Heatmap of mice in EPMT. **i**, Percentage of active time in the open arms of EPMT ($F_{2,37} = 2.409$, $P = 0.104$, planned comparison *t*-test, hM3Dq versus mCherry, $^*P = 0.013$). **j**, Percentage of entries into the open arms of EPMT ($F_{2,37} = 2.481$, $P = 0.097$, planned comparison *t*-test, hM3Dq versus mCherry, $^*P = 0.032$). **k** and **l**, Total time spent immobile in TST ($F_{2,37} = 0.891$, $P = 0.419$). **m-q**, Representative images, and quantification of c-Fos and Egr1 expression, and DCX-positive immature aDGCs in the DG (o, $F_{2,10} = 8.969$, $^*P = 0.006$; p, $F_{2,18} = 4.628$, $^*P = 0.024$; q, $F_{2,15} = 2.885$, $P = 0.087$). All scale bars are 100 μm.

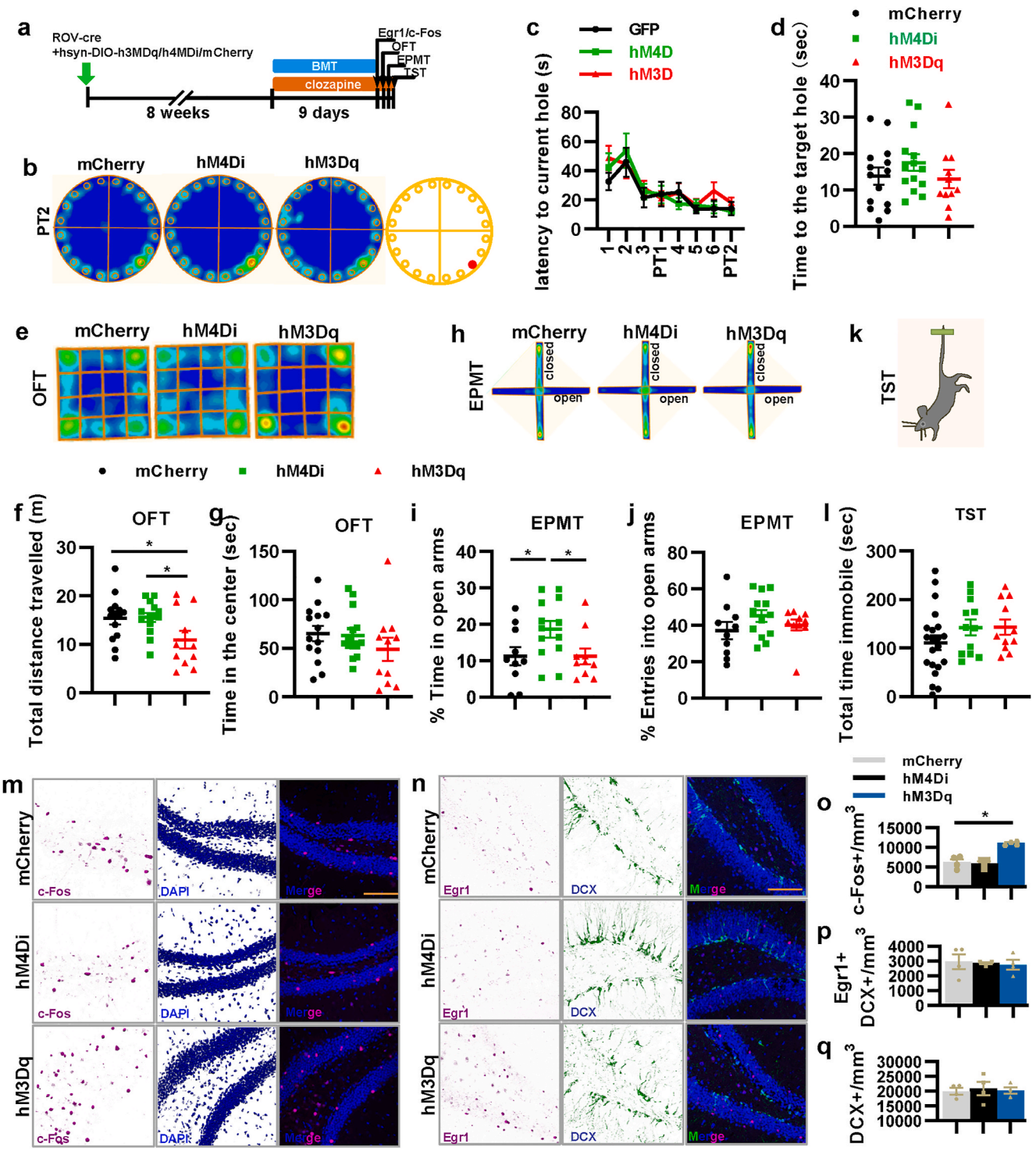

Fig. 3. The activity of 8–10-week-old new mature aDGCs does not affect spatial memory, anxiety-like behavior, as well as the excitability of mature and immature aDGCs. a, Experimental design for the behavioral tests. BMT, Barnes maze test; OFT, open field test; EPMT, elevated plus maze test; and TST, tail suspension test. **b**, The heatmap of mice in probe test 2 of BMT. **c**, Latency to the escape hole in BMT during training and in probe tests 1 and 2 (two-way ANOVA, interaction $F_{14,252} = 0.579$, $P = 0.880$; day $F_{7,252} = 8.977$, $^*P < 0.001$; virus $F_{2,36} = 0.654$, $P = 0.526$). **d**, Active time at the escape hole ($F_{2,36} = 1.012$, $P = 0.373$). **e**, Heatmap of mice in OFT. **f**, Total distance traveled in OFT ($F_{2,36} = 3.652$, $^*P = 0.036$). **g**, Active time of mice in the center of OFT ($F_{2,36} = 1.003$, $P = 0.377$). **h**, Heatmap of mice in EPMT. **i**, Percentage of active time in the open arms of EPMT ($F_{2,30} = 3.601$, $^*P = 0.040$). **j**, Percentage of entries into the open arms of EPMT ($F_{2,30} = 1.305$, $P = 0.286$). **k** and **l**, Total time spent immobile in TST ($F_{2,32} = 0.044$, $P = 0.957$). **m-q**, Representative images, and quantification of c-Fos and Egr1 expression, and DCX-positive immature aDGCs in the DG (o, $F_{2,9} = 26.389$, $^*P < 0.001$; p, $F_{2,9} = 0.096$, $P = 0.909$; q, $F_{2,9} = 0.105$, $P = 0.902$). All scale bars are 100 μm.

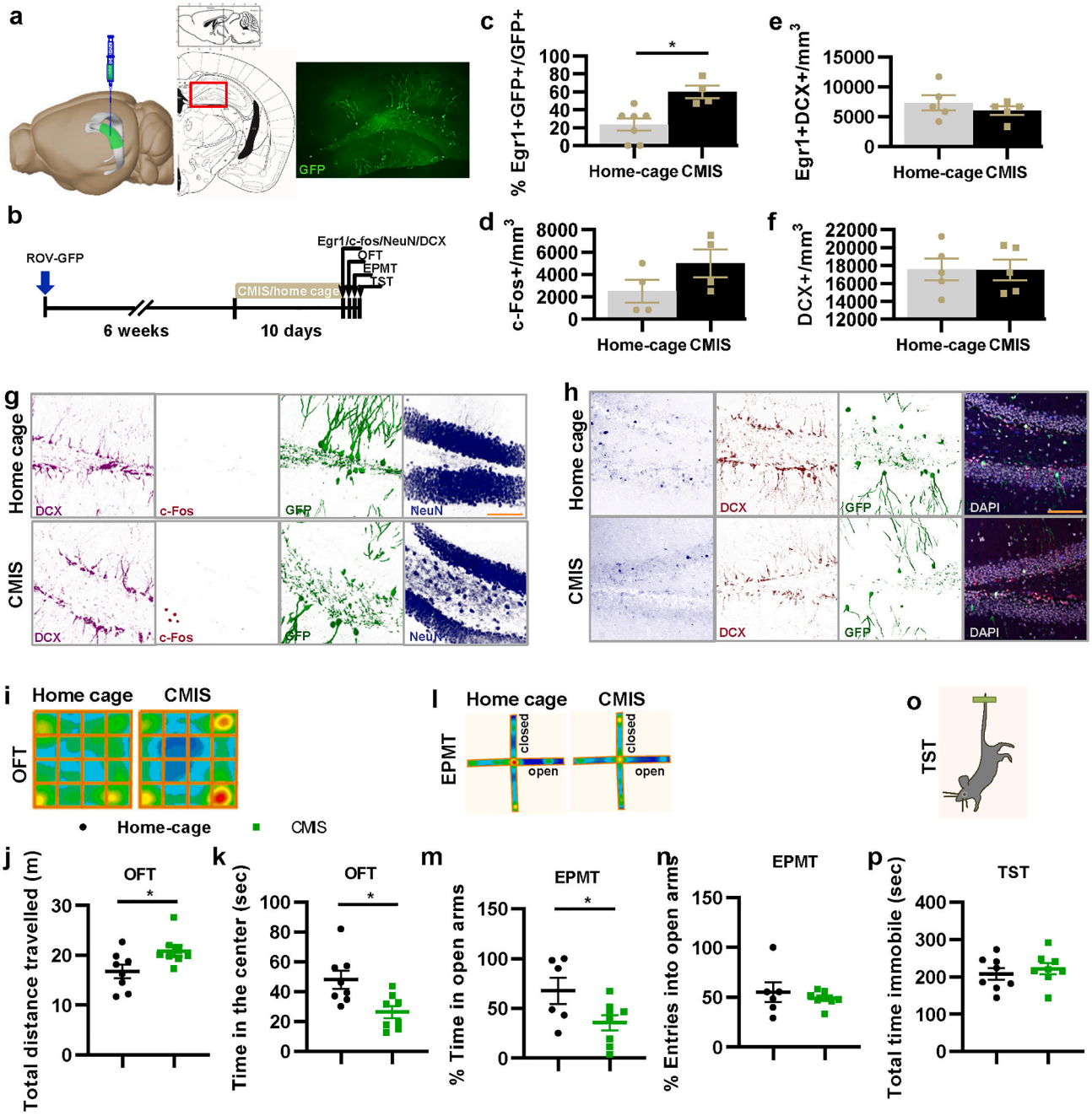

Fig. 4. Chronic mild immobility stress induced the activation of new mature aDGCs and anxiety-like behavior. a, Rov-GFP infection in DG. **b**, Experimental design for chronic mild immobility stress. **c-h**, Representative images and quantification of c-Fos and Egr1 expression, and DCX positive immature aDGC in the DG (c, $t = 3.440$, $^*P = 0.007$; d, $t = 1.567$, $P = 0.168$; e, $t = 0.912$, $P = 0.389$; f, $t = 0.050$, $P = 0.961$). **i**, Heatmap of mice in OFT. **j**, Total distance traveled in OFT ($t = 2.378$, $^*P = 0.032$). **k**, Active time of mice in the center of OFT ($t = 2.982$, $^*P = 0.010$). **l**, Heatmap of mice in EPMT. **m**, Percentage of active time in the open arms of EPMT ($t = 2.229$, $^*P = 0.046$). **n**, Percentage of entries into the open arms of EPMT ($t = 0.660$, $P = 0.522$). **o** and **p**, Total time immobile in TST ($t = 0.624$, $P = 0.543$). All scale bars are 100 μm.

week-old new mature aDGCs confers memory. Meanwhile, activation of 8–10-week-old adult born neurons did not induced anxiety-like behaviors in mice, which further indicated the key role of 6–8-week-old new mature aDGCs. Their ability to normally develop their quiet properties determines the generation of anxiety-like behavior.

Maturing aDGCs gradually enter the resting state (Ohline et al., 2018). Thus, determination of the physiological significance of the quiet property of new mature aDGCs for memory and mood may show therapeutic potential as a strategy aimed at protecting immature aDGCs in the adult brain. Here, we showed that excitation of 6–8-week-old new mature aDGCs induced anxiety-like behavior, suppressed the activity of immature aDGCs, and activated mature DG neurons, which may affect the microenvironment of DG neurogenesis (Navarro Negredo et al., 2020). The results suggest that a set of circumstances that abnormally activated new mature aDGCs generated over a long period, preventing new mature aDGCs from normally entering the resting state, may trigger the body's self-protection mechanism from this abnormal excitability by reducing neurogenesis. This may explain why depressive rodents are often accompanied by a decrease in neurogenesis (Kreisel et al., 2014; Pham et al., 2003; Schoenfeld et al., 2017).

DG plays a key role in learning and memory, and anxiety disorders (Kheirbek et al., 2013), and can be divided into dorsal and ventral DG;

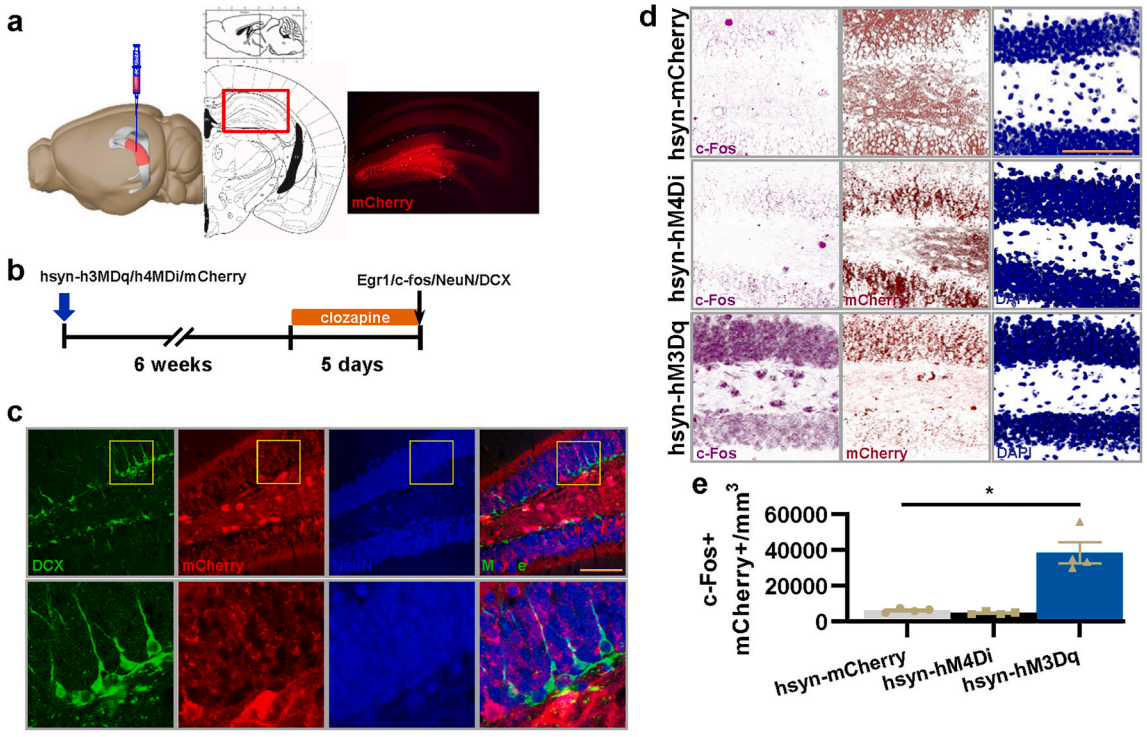

Fig. 5. Human synapsin I promoter AAV successfully expressed in and interfered with the activity of DG mature neurons. a, Expression of mCherry under the control of human synapsin I in the DG. **b**, Experimental design for efficiency detection of virus tools. **c**, Confocal images of DCX, NeuN, and mCherry show the localization of mCherry-positive neurons (arrow). **d**, Confocal photographs of c-Fos, mCherry, and DAPI show the localization of c-Fos in mCherry-positive neurons. **e**, Quantification of c-Fos and mCherry double-positive neurons in DG following a series of clozapine treatments ($F_{2,9} = 31.423$, $^*P < 0.001$). All scale bars are 100 μm.

among them, it is usually considered that dorsal DG regulates learning and memory, and ventral DG predominately regulates anxiety (Bannerman et al., 2004; Jašarević et al., 2014; Kheirbek et al., 2013; Weeden et al., 2015). Conversely, other reports show that both dorsal and ventral DG are involved in regulating memory and anxiety (Fredes et al., 2021; Günther et al., 2019; Huckleberry et al., 2018; Wang et al., 2020). In our study, a relatively large dose of virus was used to infect both dorsal and ventral DG simultaneously. As a result, we were unable to find the specific regulation role of the activity of aDGCs at a specific stage in the dorsal and ventral DG. Therefore, further research is required to show the specific function of the activity of new mature aDGCs in the dorsal and ventral hippocampus.

It has been reported that both dorsal and ventral DG optogenetic activation can induce an increase in exploratory behavior, presented as increased time in the open arms of elevated plus maze, and in motor ability, presented as increased total distance traveled in the OFT (Kheirbek et al., 2013). This is consistent with our findings that activation of DG neurons with human synapsin I promoter AAV increased exploratory behavior. Conversely, ventral DG optogenetic activation can increase the percentage of center distance in the OFT (Kheirbek et al., 2013), while our results show that activation of mature DG neurons decreased the time in the center of the open field. This may be due to several reasons. Human synapsin I promoter AAV used in our study may infect both granule cells and interneurons in the hilus. Furthermore, both dorsal and ventral DG were interfered in our experiment, and our activation cycle was longer. Therefore, these findings require further confirmation. Meanwhile, it has reported that decrease the number of neurogenesis using valganciclovir-treated TK mice, in which DCX + new born neurons almost disappeared, caused increased total immobility in TST (Snyder et al., 2011). Conversely, we found that activation of mature GCs induced decrease in the number of new born neurons to one third of the control group, and exhibited decreased total immobility in TST. This suggests that relatively low levels of neurogenesis may not be enough to produce depressive-like behavior, and enhanced motor ability induced by activation of GCs affects the performance of mice in TST.

Recently, Clozapine was proved to be more efficient and to have lower side effects on DREADD experiments than clozapine- N-oxide. According to McOmish et al. (2012), 5 mg/kg clozapine can suppress the locomotion in the open field, but have no effect on locomotion when the dosage is less than 2.5 mg/kg. Here, we used 0.4 mg/kg clozapine, which was far less than the dosage which can suppress locomotion. Conversely, the dosage of CNO required for DREADD activation is 1–10 mg/kg, and 1 mg/kg CNO can significantly decrease the locomotor activity in non-DREADD mice (Gomez et al., 2017), which may affect the accuracy of our results of measuring anxiety in OFT. Meanwhile, another report showed that CNO even at a relatively high dose is slower to generate the effect on c-Fos expression and emergence from isoflurane anesthesia (Zhou et al., 2018). Overall, we chose the higher affinity clozapine for our DREADD activation. According to previous studies (Gomez et al., 2017; Zhou et al., 2018), clozapine can induce significant changes in the DREADD activity at 40 min after injection, and this effect lasts for more than 20 min, therefore, we chose 45 min for our study similar to that reported by Zhou et al. (2018).

5. Conclusions

Our results combined showed that during the maturation of newborn neurons, their ability to directly enter the resting state at a key time window determines the anxiety-like behavior, even the depressive-like behavior, while the maintenance of normal excitation ability of new mature aDGCs confers memory. Furthermore, the anxiety mood is closely related to the excitability of various neurons, such as immature aDGCs, new mature aDGCs, and mature neurons, in the DG area. Our findings suggest that strategies aimed at inhibiting hysterical new mature aDGCs may protect against stress-related psychiatric disorders, such as anxiety and depression. However, the way to interfere with the activity of unusual hyperactive new mature aDGCs in humans remains a challenge.

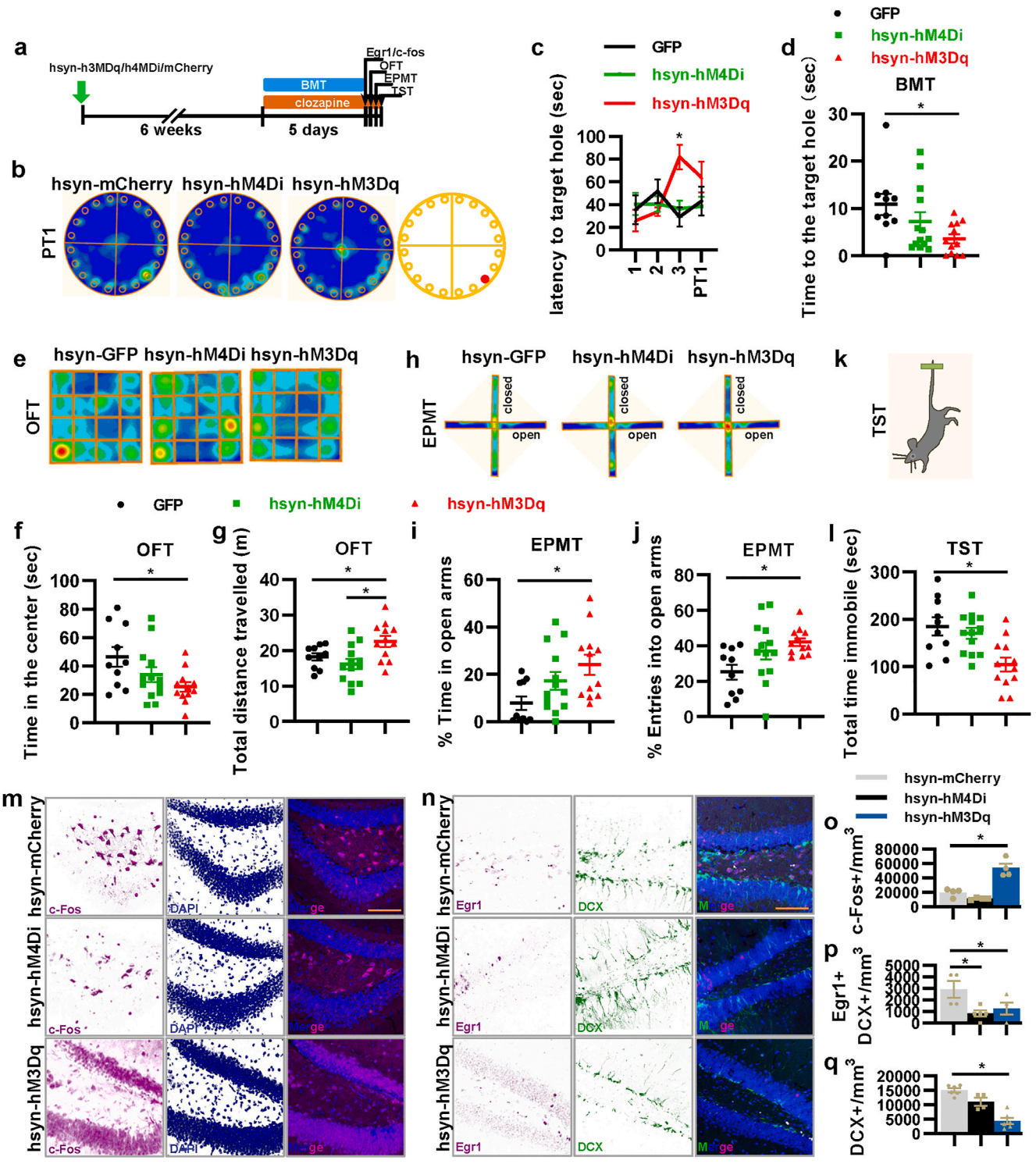

Fig. 6. The activity of DG mature neurons regulates spatial memory, anxiety-like behavior, as well as excitability of immature aDGCs. a, Experimental design for the behavioral test. **b**, Heatmap of mice in probe test 1 of BMT. **c**, Latency to the escape hole in BMT during training and in probe test 1 (two-way ANOVA, interaction $F_{6,128} = 3.391$, $P = 0.004$; day $F_{3,128} = 1.603$, $P = 0.192$; virus $F_{2,128} = 2.121$, $P = 0.124$). **d**, Active time at the escape hole (one-way ANOVA followed by a Bonferroni post-hoc test, $F_{2,32} = 3.929$, $^*P = 0.03$). **e**, Heatmap of mice in the OFT. **f**, Active time of mice in the center of the OFT ($F_{2,32} = 3.806$, $^*P = 0.033$). **g**, Total distance traveled in the OFT ($F_{2,32} = 5.755$, $^*P = 0.007$). **h**, Heatmap of mice in the EPMT. **i**, Percentage of active time in the open arms of the EPMT ($F_{2,32} = 4.298$, $^*P = 0.022$). **j**, Percentage of entries into the open arms of the EPMT ($F_{2,32} = 4.412$, $^*P = 0.020$). **k** and **l**, Total time spent immobile in TST ($F_{2,32} = 8.004$, $^*P = 0.002$). **m-q**, Representative images, and quantification of c-Fos and Egr1 expression, and DCX-positive immature aDGCs in the DG (o, $F_{2,9} = 32.540$, $^*P < 0.001$; p, $F_{2,10} = 4.663$, $^*P = 0.037$; q, $F_{2,13} = 29.458$, $^*P < 0.001$). All scale bars are 100 μm.

Disclosure

All authors report no biomedical financial interests or potential conflicts of interest.

CRediT authorship contribution statement

Guohua Wang: Conceptualization, Methodology, Formal analysis, Investigation, Data curation, Visualization, Writing – original draft, Writing – review & editing. **Canmao Wang:** Methodology, Conceptualization, Writing – review & editing. **He Chen:** Conceptualization, Methodology, Writing – review & editing. **Limei Chen:** Conceptualization, Methodology, Writing – review & editing. **Juan Li:** Conceptualization, Methodology, Supervision, Writing – original draft, Writing – review & editing, Funding acquisition.

Declaration of competing interest

The authors declare no conflict of interest.

Acknowledgements

This work was supported by the National Natural Science Foundation of China (Grant No. 81601654), Natural Science Foundation of Guangdong Province, China (Grant No. 2014A030310090 and 2016A030313578), Medical Scientific Research Foundation of Guangdong Province, China (Grant No. A2015207), Pearl River S&T Nova Program of Guangzhou (201806010037), and Scientific Research Foundation of Southern Medical University (Grant No. PY2014N001 and QD2015N001).

List of abbreviations

Adult-born dentate granule cells aDGCs
Mature granule cells GCs
Chronic mild immobilization stress CMIS
Barnes maze test BMT
Open field test OFT
Elevated plus maze test EPMT
Tail suspension test TST
Dentate gyrus DG
early growth response 1 Egr1
4′,6-diamidino-2-phenylindole DAPI
Doublecortin DCX

References

Anacker, C., Hen, R., 2017. Adult hippocampal neurogenesis and cognitive flexibility - linking memory and mood. Nat. Rev. Neurosci. 18, 335–346. https://doi.org/10.1038/nrn.2017.45.

Anacker, C., Luna, V.M., Stevens, G.S., Millette, A., Shores, R., Jimenez, J.C., Chen, B., Hen, R., 2018. Hippocampal neurogenesis confers stress resilience by inhibiting the ventral dentate gyrus. Nature 559, 98–102. https://doi.org/10.1038/s41586-018-0262-4.

Attar, A., Liu, T., Chan, W.T., Hayes, J., Nejad, M., Lei, K., Bitan, G., 2013. A shortened Barnes maze protocol reveals memory deficits at 4-months of age in the triple-transgenic mouse model of Alzheimer's disease. PloS One 8, e80355. https://doi.org/10.1371/journal.pone.0080355.

Autry, A.E., Adachi, M., Nosyreva, E., Na, E.S., Los, M.F., Cheng, P.F., Kavalali, E.T., Monteggia, L.M., 2011. NMDA receptor blockade at rest triggers rapid behavioural antidepressant responses. Nature 475, 91–95. https://doi.org/10.1038/nature10130.

Awasthi, A., Ramachandran, B., Ahmed, S., Benito, E., Shinoda, Y., 2019. Synaptotagmin-3 drives AMPA receptor endocytosis, depression of synapse strength. and forgetting 363. https://doi.org/10.1126/science.aav1483.

Bannerman, D.M., Rawlins, J.N., McHugh, S.B., Deacon, R.M., Yee, B.K., Bast, T., Zhang, W.N., Pothuizen, H.H., Feldon, J., 2004. Regional dissociations within the hippocampus–memory and anxiety. Neurosci. Biobehav. Rev. 28, 273–283. https://doi.org/10.1016/j.neubiorev.2004.03.004.

Beining, M., Jungenitz, T., Radic, T., Deller, T., Cuntz, H., Jedlicka, P., Schwarzacher, S. W., 2017. Adult-born dentate granule cells show a critical period of dendritic reorganization and are distinct from developmentally born cells. Brain Struct. Funct. 222, 1427–1446. https://doi.org/10.1007/s00429-016-1285-y.

Can, A., Dao, D.T., Terrillion, C.E., Piantadosi, S.C., Bhat, S., Gould, T.D., 2012. The tail suspension test. JoVE : JoVE, e3769. https://doi.org/10.3791/3769.

Cho, K.O., Lybrand, Z.R., Ito, N., Brulet, R., Tafacory, F., Zhang, L., Good, L., Ure, K., Kernie, S.G., Birnbaum SGet al, 2015. Aberrant hippocampal neurogenesis contributes to epilepsy and associated cognitive decline. Nat. Commun. 6, 6606. https://doi.org/10.1038/ncomms7606.

Choi, S.H., Bylykbashi, E., Chatila, Z.K., Lee, S.W., Pulli, B., Clemenson, G.D., Kim, E., Rompala, A., Oram, M.K., Cet al, Asselin, 2018. Combined Adult Neurogenesis and BDNF Mimic Exercise Effects on Cognition in an Alzheimer's Mouse Model, vol. 361. Science, New York, NY. https://doi.org/10.1126/science.aan8821.

Cole, J.D., Espinueva, D.F., Seib, D.R., Ash, A.M., Cooke, M.B., Cahill, S.P., O'Leary, T.P., Kwan, S.S., Snyder, J.S., 2020. Adult-born hippocampal neurons undergo extended development and are morphologically distinct from neonatally-born neurons. J. Neurosci. : the official journal of the Society for Neuroscience 40, 5740–5756. https://doi.org/10.1523/jneurosci.1665-19.2020.

Drew, L.J., Kheirbek, M.A., Luna, V.M., Denny, C.A., Cloidt, M.A., Wu, M.V., Jain, S., Scharfman, H.E., Hen, R., 2016. Activation of local inhibitory circuits in the dentate gyrus by adult-born neurons. Hippocampus 26, 763–778. https://doi.org/10.1002/hipo.22557.

Fredes, F., Silva, M.A., Koppensteiner, P., Kobayashi, K., Joesch, M., Shigemoto, R., 2021. Ventro-dorsal hippocampal pathway gates novelty-induced contextual memory formation. Curr. Biol. : Cailiao Baohu 31, 25–38. https://doi.org/10.1016/j.cub.2020.09.074 e25.

Günther, A., Luczak, V., Gruteser, N., Abel, T., Baumann, A., 2019. HCN4 knockdown in dorsal hippocampus promotes anxiety-like behavior in mice. Gene Brain Behav. 18 https://doi.org/10.1111/gbb.12550 e12550-e12550.

Ge, S., Yang, C.H., Hsu, K.S., Ming, G.L., Song, H., 2007. A critical period for enhanced synaptic plasticity in newly generated neurons of the adult brain. Neuron 54, 559–566. https://doi.org/10.1016/j.neuron.2007.05.002.

Gomez, J.L., Bonaventura, J., Lesniak, W., Mathews, W.B., Sysa-Shah, P., Rodriguez, L. A., Ellis, R.J., Richie, C.T., Harvey, B.K., RFet al, Dannals, 2017. Chemogenetics Revealed: DREADD Occupancy and Activation via Converted Clozapine, vol. 357. Science, New York, NY, pp. 503–507. https://doi.org/10.1126/science.aan2475.

Gu, Y., Arruda-Carvalho, M., Wang, J., Janoschka, S.R., Josselyn, S.A., Frankland, P.W., Ge, S., 2012. Optical controlling reveals time-dependent roles for adult-born dentate granule cells. Nat. Neurosci. 15, 1700–1706. https://doi.org/10.1038/nn.3260.

Horgusluoglu, E., Nudelman, K., Nho, K., Saykin, A.J., 2017. Adult neurogenesis and neurodegenerative diseases: a systems biology perspective. Am. J. Med. Genet. Part B, Neuropsychiatric genetics : the official publication of the International Society of Psychiatric Genetics 174, 93–112. https://doi.org/10.1002/ajmg.b.32429.

Huckleberry, K.A., Shue, F., Copeland, T., Chitwood, R.A., Yin, W., Drew, M.R., 2018. Dorsal and ventral hippocampal adult-born neurons contribute to context fear memory. Neuropsychopharmacology : official publication of the American College of Neuropsychopharmacology 43, 2487–2496. https://doi.org/10.1038/s41386-018-0109-6.

Jašarević, E., Hecht, P.M., Fritsche, K.L., Beversdorf, D.Q., Geary, D.C., 2014. Dissociable effects of dorsal and ventral hippocampal DHA content on spatial learning and anxiety-like behavior. Neurobiol. Learn. Mem. 116, 59–68. https://doi.org/10.1016/j.nlm.2014.08.009.

Jungenitz, T., Radic, T., Jedlicka, P., Schwarzacher, S.W., 2014. New York, NY : 1991. High-frequency Stimulation Induces Gradual Immediate Early Gene Expression in Maturing Adult-Generated Hippocampal Granule Cells. Cerebral Cortex, vol. 24, pp. 1845–1857. https://doi.org/10.1093/cercor/bht035.

Kajimoto, K., Valenzuela, C.F., Allan, A.M., Ge, S., Gu, Y., Cunningham, L.A., 2016. Prenatal alcohol exposure alters synaptic activity of adult hippocampal dentate granule cells under conditions of enriched environment. Hippocampus 26, 1078–1087. https://doi.org/10.1002/hipo.22588.

Kerloch, T., Clavreul, S., Goron, A., Abrous, D.N., Pacary, E., 2019. Dentate Granule Neurons Generated during Perinatal Life Display Distinct Morphological Features Compared with Later-Born Neurons in the Mouse Hippocampus. Cerebral Cortex, vol. 29, pp. 3527–3539. https://doi.org/10.1093/cercor/bhy224. New York, NY : 1991.

Kheirbek, M.A., Drew, L.J., Burghardt, N.S., Costantini, D.O., Tannenholz, L., Ahmari, S. E., Zeng, H., Fenton, A.A., Hen, R., 2013. Differential control of learning and anxiety along the dorsoventral axis of the dentate gyrus. Neuron 77, 955–968. https://doi.org/10.1016/j.neuron.2012.12.038.

Kreisel, T., Frank, M.G., Licht, T., Reshef, R., Ben-Menachem-Zidon, O., Baratta, M.V., Maier, S.F., Yirmiya, R., 2014. Dynamic microglial alterations underlie stress-induced depressive-like behavior and suppressed neurogenesis. Mol. Psychiatr. 19, 699–709. https://doi.org/10.1038/mp.2013.155.

Kropff, E., Yang, S.M., Schinder, A.F., 2015. Dynamic role of adult-born dentate granule cells in memory processing. Curr. Opin. Neurobiol. 35, 21–26. https://doi.org/10.1016/j.conb.2015.06.002.

Kuhn, H.G., Toda, T., Gage, F.H., 2018. Adult hippocampal neurogenesis: a coming-of-age story. J. Neurosci. : the official journal of the Society for Neuroscience 38, 10401–10410. https://doi.org/10.1523/jneurosci.2144-18.2018.

Kurawa, M.I., Magaji, R.A., Yusuf, T., Magaji, M.G., 2020. Effects of mosquito coil smoke inhalation on spatial memory in mice. Niger. J. Physiol. Sci. : official publication of the Physiological Society of Nigeria 35, 68–76.

McOmish, C.E., Lira, A., Hanks, J.B., Gingrich, J.A., 2012. Clozapine-induced locomotor suppression is mediated by 5-HT2A receptors in the forebrain. Neuropsychopharmacology : official publication of the American College of Neuropsychopharmacology 37, 2747–2755. https://doi.org/10.1038/npp.2012.139.

Navarro Negredo, P., Yeo, R.W., Brunet, A., 2020. Aging and rejuvenation of neural stem cells and their niches. Cell stem cell 27, 202–223. https://doi.org/10.1016/j.stem.2020.07.002.

Ohline, S.M., Wake, K.L., Hawkridge, M.V., Dinnunhan, M.F., Hegemann, R.U., Wilson, A., Schoderboeck, L., Logan, B.J., Jungenitz, T., Schwarzacher SWet al, 2018. Adult-born dentate granule cell excitability depends on the interaction of neuron age, ontogenetic age and experience. Brain Struct. Funct. 223, 3213–3228. https://doi.org/10.1007/s00429-018-1685-2.

Park, S.C., 2019. Neurogenesis and antidepressant action. Cell Tissue Res. 377, 95–106. https://doi.org/10.1007/s00441-019-03043-5.

Pham, K., Nacher, J., Hof, P.R., McEwen, B.S., 2003. Repeated restraint stress suppresses neurogenesis and induces biphasic PSA-NCAM expression in the adult rat dentate gyrus. Eur. J. Neurosci. 17, 879–886. https://doi.org/10.1046/j.1460-9568.2003.02513.x.

Piatti, V.C., Davies-Sala, M.G., Espósito, M.S., Mongiat, L.A., Trinchero, M.F., Schinder, A.F., 2011. The timing for neuronal maturation in the adult hippocampus is modulated by local network activity. J. Neurosci. : the official journal of the Society for Neuroscience 31, 7715–7728. https://doi.org/10.1523/jneurosci.1380-11.2011.

Pitts, M.W., 2018. Barnes maze procedure for spatial learning and memory in mice. Bio-protocol 8. https://doi.org/10.21769/bioprotoc.2744.

Planchez, B., Surget, A., Belzung, C., 2020. Adult hippocampal neurogenesis and antidepressants effects. Curr. Opin. Pharmacol. 50, 88–95. https://doi.org/10.1016/j.coph.2019.11.009.

Ramirez, S., Liu, X., MacDonald, C.J., Moffa, A., Zhou, J., Redondo, R.L., Tonegawa, S., 2015. Activating positive memory engrams suppresses depression-like behaviour. Nature 522, 335–339. https://doi.org/10.1038/nature14514.

Rosenfeld, C.S., Ferguson, S.A., 2014. Barnes maze testing strategies with small and large rodent models. JoVE : JoVE, e51194. https://doi.org/10.3791/51194.

Schoenfeld, T.J., McCausland, H.C., Morris, H.D., Padmanaban, V., Cameron, H.A., 2017. Stress and loss of adult neurogenesis differentially reduce hippocampal volume. Biol. Psychiatr. 82, 914–923. https://doi.org/10.1016/j.biopsych.2017.05.013.

Snyder, J.S., Soumier, A., Brewer, M., Pickel, J., Cameron, H.A., 2011. Adult hippocampal neurogenesis buffers stress responses and depressive behaviour. Nature 476, 458–461. https://doi.org/10.1038/nature10287.

Toda, T., Parylak, S.L., Linker, S.B., Gage, F.H., 2019. The role of adult hippocampal neurogenesis in brain health and disease. Mol. Psychiatr. 24, 67–87. https://doi.org/10.1038/s41380-018-0036-2.

Tunc-Ozcan, E., Peng, C.Y., Zhu, Y., Dunlop, S.R., Contractor, A., Kessler, J.A., 2019. Activating newborn neurons suppresses depression and anxiety-like behaviors. Nat. Commun. 10, 3768. https://doi.org/10.1038/s41467-019-11641-8.

van Praag, H., Schinder, A.F., Christie, B.R., Toni, N., Palmer, T.D., Gage, F.H., 2002. Functional neurogenesis in the adult hippocampus. Nature 415, 1030–1034. https://doi.org/10.1038/4151030a.

Vu, P.A., Tucker, L.B., Liu, J., McNamara, E.H., Tran, T., Fu, A.H., Kim, Y., McCabe, J.T., 2018. Transient disruption of mouse home cage activities and assessment of orexin immunoreactivity following concussive- or blast-induced brain injury. Brain Res. 1700, 138–151. https://doi.org/10.1016/j.brainres.2018.08.034.

Wang, C., Liu, H., Li, K., Wu, Z.Z., Wu, C., Yu, J.Y., Gong, Q., Fang, P., Wang, X.X., Duan, SMet al, 2020. Tactile modulation of memory and anxiety requires dentate granule cells along the dorsoventral axis. Nat. Commun. 11, 6045. https://doi.org/10.1038/s41467-020-19874-8.

Wang, G., Cheng, Y., Gong, M., Liang, B., Zhang, M., Chen, Y., Zhang, C., Yuan, X., Xu, J., 2013. Systematic correlation between spine plasticity and the anxiety/depression-like phenotype induced by corticosterone in mice. Neuroreport 24, 682–687. https://doi.org/10.1097/WNR.0b013e32836384db.

Weeden, C.S., Roberts, J.M., Kamm, A.M., Kesner, R.P., 2015. The role of the ventral dentate gyrus in anxiety-based behaviors. Neurobiol. Learn. Mem. 118, 143–149. https://doi.org/10.1016/j.nlm.2014.12.002.

Zhao, C., Teng, E.M., Summers Jr., R.G., Ming, G.L., Gage, F.H., 2006. Distinct morphological stages of dentate granule neuron maturation in the adult mouse hippocampus. J. Neurosci. : the official journal of the Society for Neuroscience 26, 3–11. https://doi.org/10.1523/jneurosci.3648-05.2006.

Zhou, W., Cheung, K., Kyu, S., Wang, L., Guan, Z., Kurien, P.A., Bickler, P.E., Jan, L.Y., 2018. Activation of orexin system facilitates anesthesia emergence and pain control. Proc. Natl. Acad. Sci. U.S.A. 115, E10740–e10747. https://doi.org/10.1073/pnas.1808622115.